PERGAMON

Available online at www.sciencedirect.com

SCIENCE DIRECT®

Vision Research 43 (2003) 2707–2719

Vision Research

www.elsevier.com/locate/visres

Contrast coding and magno/parvo segregation revealed in reaction time studies

I.J. Murray [a,*], S. Plainis [b]

[a] Visual Sciences Laboratory, Department of Optometry and Neuroscience, UMIST, P.O. Box 88, Manchester M60 1QD, UK

[b] VEIC, Division of Ophthalmology, School of Medicine, University of Crete, P.O. Box 1352, Heraklion, Crete, Greece

Received 5 July 2002; received in revised form 17 April 2003

Abstract

Reaction times (RTs) are obtained for a wide range of contrasts of vertical sinusoidal gratings. The data are plotted as a function of the reciprocal of contrast. In some conditions, a single linear function accounts for the data. In others a clear bi-linear function is obtained. The low and high contrast regions of the function are interpreted as representing magno and parvo activity, respectively. RT-based supra-threshold sensitivity functions are obtained for different luminances, stimulus durations and eccentricities and these are compared with conventional threshold-based sensitivities to establish the extent to which RTs and contrast sensitivity are constrained by the same sensory processes.

Keywords: Parvo-cellular; Magno-cellular; Reaction times; Sinusoidal gratings; Contrast spatial frequency

1. Introduction

There is an extensive literature linking contrast, spatial frequency and simple RTs (e.g. Breitmeyer, 1975; Burkhardt, Gottesman, & Keeman, 1987; Felipe, Buades, & Artigas, 1993; Hartwell & Cowan, 1993; Harwerth & Levi, 1978; Menees, 1998; Mihaylova, Stomonyakov, & Vassilev, 1999; Parker, 1980; Thomas, Fagerholm, & Bonnet, 1999; Tolhurst, 1975; Vassilev & Mitov, 1976). For the most part, studies have concentrated on the increase in RT with spatial frequency (Breitmeyer, 1975; Felipe et al., 1993; Lupp, Hauske, & Wolf, 1976; Rudd, 1988; Totev & Mitov, 2000; Vassilev & Mitov, 1976). Although this observation is intuitively attractive, it is not easily explained in terms of our understanding of the early processing of spatial information in the primary visual pathway. On the other hand, the neural basis of early achromatic contrast coding is well developed (e.g. Bauer, Scholz, Levitt, Obermayer, & Lund, 1999; Kaplan & Shapley, 1976; Purpura, Tranchina, Kaplan, & Shapley, 1990). Furthermore, there is a systematic link between RTs and achromatic contrast as shown in many of the above papers. In the present paper we explore this relationship in order to understand better the neural basis of RTs.

Breitmeyer (1975) showed that RTs are longer for high than for low spatial frequencies, even though equal apparent contrast is used. In fact, whatever strategy is followed to compensate for the fall-off in sensitivity at higher spatial frequencies (Felipe et al., 1993; Lupp et al., 1976; Musselwhite & Jeffreys, 1985; Totev & Mitov, 2000; Vassilev & Mitov, 1976), RTs always increase with spatial frequency. Some have considered that the role of low spatial frequency channels, (transient, therefore, short RTs) and high spatial frequency channels (sustained, therefore, slow RTs) explained their data. This interpretation ignores the important point that simply adding physical contrast to higher spatial frequencies cannot compensate for low sensitivity. Sensitivity is influenced by the spatio-temporal frequency content of the stimulus but mainly it arises from the contrast gain (the increase of the response per unit change in contrast) of the underlying detecting mechanisms.

In most RT experiments, abrupt stimulus onsets are used and there can be little doubt that this introduces an inherent bias toward transient mechanisms. Tolhurst (1975) used temporally ramped stimuli to illustrate this point. He and others (Murray & Parry, 1998; Schwartz,

* Corresponding author. Tel./fax: +44-161-2003862.
E-mail address: mjcijm@fsl.op.umist.ac.uk (I.J. Murray).

0042-6989/$ - see front matter © 2003 Elsevier Ltd. All rights reserved.
doi:10.1016/S0042-6989(03)00408-5

1992) have shown that the activity of transient and sustained mechanisms is revealed in the shape of the RT frequency histogram for near-threshold grating patterns; high spatial frequency achromatic and chromatic gratings are mediated by relatively slow (sustained) temporal mechanisms and the resulting RT frequency histogram is unimodal, whereas the RT histogram of a stimulus mediated by transient mechanisms is bimodal, i.e. RTs are grouped around the onset and the offset of the stimulus.

The above experiments used mainly low contrast gratings, but it is important to test a wide range of contrasts, because, as first shown by Harwerth and Levi (1978), there is an intriguing bi-modal relationship between RTs and grating contrast. Generally, the increase in RT with the decrease of stimulus intensity is exponential and can be described by Piéron's law ($\tau - \tau_0 = \beta I^{-\alpha}$, where τ is the reaction time (RT), τ_0 is the asymptotic RT, β is a free parameter, I is the intensity of the stimulus and α is the exponent of the function; see Mansfield, 1973; Piéron, 1952; Pins & Bonet, 2000). However, when contrast is the dependent variable, Harwerth and Levi (1978) and Harwerth, Boltz, and Smith III (1980) obtained a two-phase RT vs. contrast function with some spatial frequencies. The faster RTs correspond to the relatively flat, high contrast portion of the function. They interpreted this as revealing the operation of transient mechanisms at high contrast and sustained mechanisms at low contrast. They supposed that because shorter RTs were obtained at higher contrasts, these conditions favoured transient detectors. The same conclusion was reached by Felipe et al. (1993) who reported similar RT-contrast functions. These observations have been re-interpreted in the light of the background neurophysiology (Parry, 2001; Plainis & Murray, 2000). As discussed in detail in the next paragraph, it is now generally accepted that the detection of low contrast stimuli is mediated predominantly by the magnocellular (M) pathway. Hence, it seems likely that, even though these are relatively slow, the RTs in the low contrast segment of the RT vs. contrast function are dominated by the activity of M neurons. Interestingly, Parry, Kulikowski, Murray, Kranda, and Ott (1988) also produced convincing evidence of the existence of two sections in the RT vs. achromatic contrast function, but not in the equivalent isoluminant chromatic function, where only one mechanism, the P pathway, is known to mediate the detection of the stimulus.

The above observations and many other psychophysical experiments (e.g. Burbeck & Kelly, 1981; Gegenfurtner & Hawken, 1996; Legge, 1978; Pokorny & Smith, 1997) provide unambiguous evidence of two detecting mechanisms in the early stages of the visual pathway. This notion is strongly supported by many anatomical and neurophysiological studies (Bauer et al., 1999; Lee, 1996; Lund, Wu, Hadingham, & Levitt, 1995; Perry, Oehler, & Cowey, 1984; Purpura et al., 1990; Rodieck, Binmoeller, & Dineen, 1985; Wiesel & Hubel, 1966), which have shown that visual signals are processed along two anatomically and functionally distinct pathways carrying complementary information. Neurons in the M pathway specialize in extracting luminance contrast and fast flicker, whilst parvocellular (P) neurons have relatively poor sensitivity to achromatic contrast but specialize in extracting colour and, high spatial frequency information (Lee, Pokorny, Smith, Martin, & Valberg, 1990; Purpura et al., 1990; Shapley & Hawken, 1999; Yeh, Lee, & Kremers, 1995). The most conspicuous, and universally recognised difference between M and P neurons in neurophysiological experiments is their processing of luminance contrast: M neurons have high luminance contrast sensitivity, exhibit correspondingly high contrast gain (they respond vigorously to small changes in contrast), but saturate at fairly low contrasts; P neurons have low contrast gain, but show a high degree of spatial and temporal linearity (Derrington & Lennie, 1984; Hicks, Lee, & Vidyasagar, 1983; Kaplan, Lee, & Shapley, 1990; Kaplan & Shapley, 1982; Kaplan & Shapley, 1986; Lee, 1996; Lee et al., 1990; Purpura, Kaplan, & Shapley, 1988; Sclar, Maunsell, & Lennie, 1990).

In fact, it can be argued that contrast gain is proportional to contrast sensitivity (Kaplan & Shapley, 1986). Hence, in hindsight we can speculate that the different regions of the RT vs. contrast function, may represent the activities of mechanisms having differing contrast gains. In the experiments described here we test this idea using an RT equivalent of contrast gain, shown previously (Murray & Plainis, 2000; Plainis & Murray, 2000) to correspond closely to the physiologically determined values for M and P pathways. Secondly, RT data are transformed to produce sensitivity functions with varying luminance levels, eccentricity and stimulus duration, in order to establish whether RT-based contrast coding and contrast sensitivity are constrained by the same neural processes. Both of these strategies have the same aim—to determine the link between RTs and the neural mechanisms in the early stages of visual processing.

2. Methods

2.1. Stimuli

The stimuli were vertical sinusoidal gratings, modulated in luminance, and displayed on a Barco CCID7651 'Calibrator' colour monitor. The red, green and sync inputs to the monitor were supplied by a 12-bit, two-channel grating generator card (Millipede Prisma VR1000 series 2) in a PC. The red and green guns of the monitors were combined in phase to produce a yellowish background (co-ordinates on the chromaticity diagram:

$x = 0.508$; $y = 0.437$ measured with a Spectrascan Photo Research 650 colorimeter, Micron Ltd., London), which was periodically replaced by the grating with no change in mean hue or luminance. Refresh rate was 100 Hz. The mean luminance of the screen $[L = (L_{max} + L_{min})/2]$ was 20 cd/m^2, and this was attenuated with neutral density filters to give lower luminances. The surround was dark. The test field was the central area of the monitor, the peripheral area of which was occluded by black card. The circular target subtended an angle of 7.13 deg at a viewing distance of 114 cm. The minimum number of cycles presented on the screen was 3.5 for the lowest spatial frequency used (0.49 c/deg). Normal pupils were used apart from one control experiment. Pupil size was measured for different ranges of luminances for each subject. Subjects fixated on a cross located in the centre of the illuminated area of the screen for central viewing and on a series of red LEDs when eccentric viewing was tested. Contrast and luminance were frequently measured with a PR1500 photometer (Micron Ltd., London).

RT data were collected for a range of contrasts from suprathreshold (0.5) to threshold (C_0) detection. Contrast was defined after Michelson:

$$C = (L_{max} - L_{min})/(L_{max} + L_{min}),$$

where L_{max} = maximum luminance and L_{min} = minimum luminance. A series of spatial frequencies (0.49–17.7 c/deg) and mean luminances (20–0.005 cd/m^2) were used. Eccentricities of 0, 5, 10 and 15 deg for both hemifields were tested. Generally stimuli were presented for 340 ms. In some experiments stimulus duration varied between 20, 50 and 500 ms.

2.2. Procedure

RTs were determined using a CED 1401 smart interface (1 ms temporal resolution), linked to a PC, and a purpose-designed computer programme. They were measured by displaying vertical gratings with an abrupt onset and offset. Subjects responded by pressing a button which triggered the interface (CED 1401). Before the RT measurement procedure began, the subjects adapted to the particular level of luminance for between 5 and 15 min. A trial (a block of 32 presentations of the corresponding grating) consisted of the following sequence of events. A single warning tone was sounded. This was followed by a random foreperiod varying from 1000 to 3000 ms prior to the presentation of the target stimulus. At the onset of the grating, a trigger probe was set which prompted the CED 1401 to start its integral clock counter. The subject was instructed to press the response button immediately he/she detected the stimulus; the response button terminated the clock counter. A time-out occurred if there was no response within 2000 ms. Only responses between 150 and 1000 ms were accepted; RTs over 600 ms were rarely encountered.

2.3. Subjects

Three young subjects (SP, LG and NH) were used. Subjects were familiarised with the range of conditions to be used in the experiment and were given a block of practice trials prior to RT recording in which different sets of spatial frequencies were presented. The subjects were optically corrected for the viewing distance with spectacles (corrected VA = 6/5) and viewed the stimuli through natural pupils and binocularly.

3. Results

In Fig. 1(a) RT data for one condition (11.22 c/deg, 50 ms duration, Subject LG) are plotted as a function of contrast on a logarithmic axis. It is evident that RTs decrease exponentially as contrast is increased. As was previously shown (Plainis & Murray, 2000), the RT vs. contrast curves can be described satisfactorily by the following monotonic function:

$$\tau = \tau_0 + \beta \cdot C^{-1} \quad (1)$$

This is a Piéron function (described in Section 1) with the exponent α being equal to -1, where τ is the measured RT, τ_0 is the asymptotic RT reached at the highest contrasts (comprising motor time and other non-visual factors), β is a constant (characterizing the steepness of the curve) and C is Michelson contrast.

From Eq. (1) it follows that, if the data are re-plotted in terms of $1/C$, the resulting slope, k, would be linear, as is confirmed in Fig. 1(b) ($r^2 = 0.997$). This relationship is extremely robust for many observers and a wide range of stimulus conditions (e.g. luminance, spatial frequency), as shown in Plainis and Murray (2000).

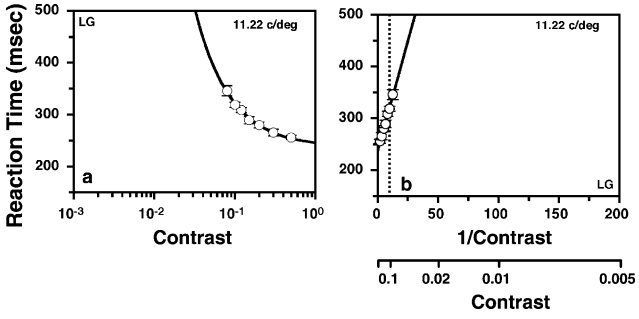

Fig. 1. Plots of RT vs. contrast (a) and vs. the reciprocal of contrast (b) for subject LG and for a specific stimulus (spatial frequency: 11.22 c/deg, duration: 50 ms, luminance: 20 cd/m^2). Each data point represents the mean of at least 24 measurements (maximum = 32) and the error bars ±1 s.e. The solid line drawn through the data is the best fit of Eq. (1) (a), or the least square regression fit (b). The vertical dotted line indicates $C = 0.1$.

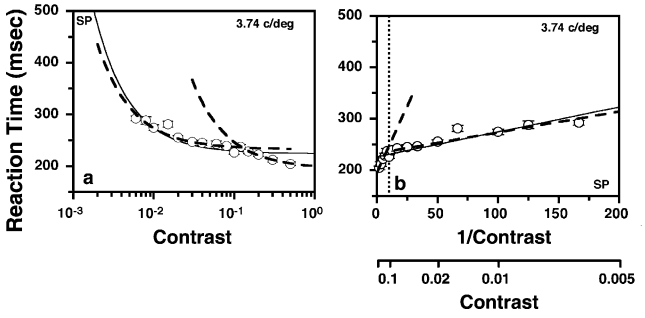

Fig. 2. Plots of RT vs. contrast (a) and vs. the reciprocal of contrast (b) for subject SP and for a specific stimulus (spatial frequency: 3.74 c/deg, duration: 500 ms, luminance: 20 cd/m^2) which produces a biphasic function. Each data point represents the mean of at least 24 measurements (maximum = 32) and the error bars ±1 s.e. The dashed lines drawn through the data are the best fits of Eq. (1) (a) or the least square regression fits (b) for high contrast levels (0.5–0.1) and low contrast levels (0.1 to threshold). The solid lines are the fits for all the data points. The vertical dotted line indicates $C = 0.1$.

However, some stimulus conditions produce a bilinear function. For example, as seen in Fig. 2(a), RTs decrease as contrast is increased, but tend to level off producing an asymptote at around $C = 0.1$. As C increases, RTs again reduce, as if a different detection mechanism operates. The break is more obvious in Fig. 2(b), where RTs are plotted as a function of $1/C$. This observation confirms previous findings (Harwerth & Levi, 1978; Harwerth et al., 1980; Parry, 2001; Parry et al., 1988). The solid line in Fig. 2(b) is the least square regression fit for all data points and the dashed bold lines are the least square regression fits for the two segments (below and above 0.1, respectively). There are two points to note from these data; first, the slope of the high contrast region is much steeper than for the low contrast region, and second, the overall slope, k, is determined by the low contrast region, as illustrated by the proximity of the solid line to the dashed line in the low contrast region. In subsequent figures, solid lines are best fit regression lines for the full contrast range and dashed lines are fits to the low and high contrast segments.

The Piéron function (1), used to model RTs is identical to the well-known Naka–Rushton equation, if the reciprocal of RT is given as a function of contrast (C):

$$\tau^{-1} = \frac{1}{(\tau_0 + k \cdot C^{-1})} = \frac{\tau_0^{-1} \cdot C}{(C + k \cdot \tau_0^{-1})} \quad (2)$$

RTs are reciprocally related to sensitivity; RTs to high suprathreshold targets are short and those to close-to-threshold targets are longer. The Naka–Rushton equation is frequently used to describe the contrast-response functions of neurons in the visual pathway (e.g. Kaplan & Shapley, 1986; Sclar et al., 1990). In this way RTs can be linked to response amplitudes and gain characteristics of P and M cells. Moreover, contrast gain, the slope of the Naka–Rushton function at 0% contrast, is used to describe sensitivity of cells.

The slope of the Naka–Rushton function (2) at contrast C is:

$$(\tau^{-1}(C)) = \frac{\tau_0^{-1}}{(C + k \cdot \tau_0^{-1})} - \frac{\tau_0^{-1} \cdot C}{(C + k \cdot \tau_0^{-1})}$$

The slope at 0% contrast is:

$$(\tau^{-1}(0)) = \frac{\tau_0^{-1}}{k \cdot \tau_0^{-1}} = k^{-1}$$

Thus, k^{-1} is an index of sensitivity (the gain) of the underlying detecting mechanism: steep slopes indicate low gain and consequently low sensitivity, shallow slopes indicate high gain (i.e. high sensitivity). It characterises the link between contrast and RT for each of the different stimulus conditions.

Fig. 3 shows the effect of spatial frequency on RT as a function of $1/C$ for two stimulus durations, 20 ms (Fig. 3(a)) and 500 ms (Fig. 3(b)). Data for subject SP only are shown, but similar results have been obtained for subject LG and not shown for brevity. First, the overall slopes (see solid lines) of the functions and their significance are described. For the short (20 ms) stimulus duration (Fig. 3(a)), k becomes steeper as spatial frequency increases (and as sensitivity decreases). At low spatial frequencies, where small increments/decrements in contrast influence RT very little, the values of k are low (high sensitivity), whereas at high spatial frequencies, where small increments/decrements have a large effect on RT, the values of k are high (low sensitivity). It is evident that in this case k gradually and systematically increases (i.e. sensitivity decreases), reaching a maximum at 11.22 c/deg.

Fig. 3(b) illustrates RT vs. $1/C$ for stimulus durations of 500 ms. Again, the slope is shallow at the lowest spatial frequencies but instead of increasing as spatial frequency increases, as in Fig. 3(a), it reduces for the first four spatial frequencies reaching a minimum (highest sensitivity) at 2.51 c/deg and then increasing to a maximum (lowest sensitivity) at 11.22 c/deg.

Turning now to the dashed lines which are least square regressions for the high and low contrast regions of the curves, the discontinuity in the RT vs. $1/C$ function is highly conspicuous for certain stimulus conditions. Note that for all conditions the break occurs around contrast 0.1 as shown by previous authors for RTs (Felipe et al., 1993; Harwerth & Levi, 1978; Parry, 2001; Parry et al., 1988) and VEPs (Hartwell & Cowan, 1993; Murray & Kulikowski, 1983; Murray, Parry, Varden, & Kulikowski, 1987; Rudvin, Valberg, & Kilavik, 2000). Values k_1 and k_2 which depict the slopes for the high and low contrast regions, respectively, are given in the top left-hand corner of each panel. When the

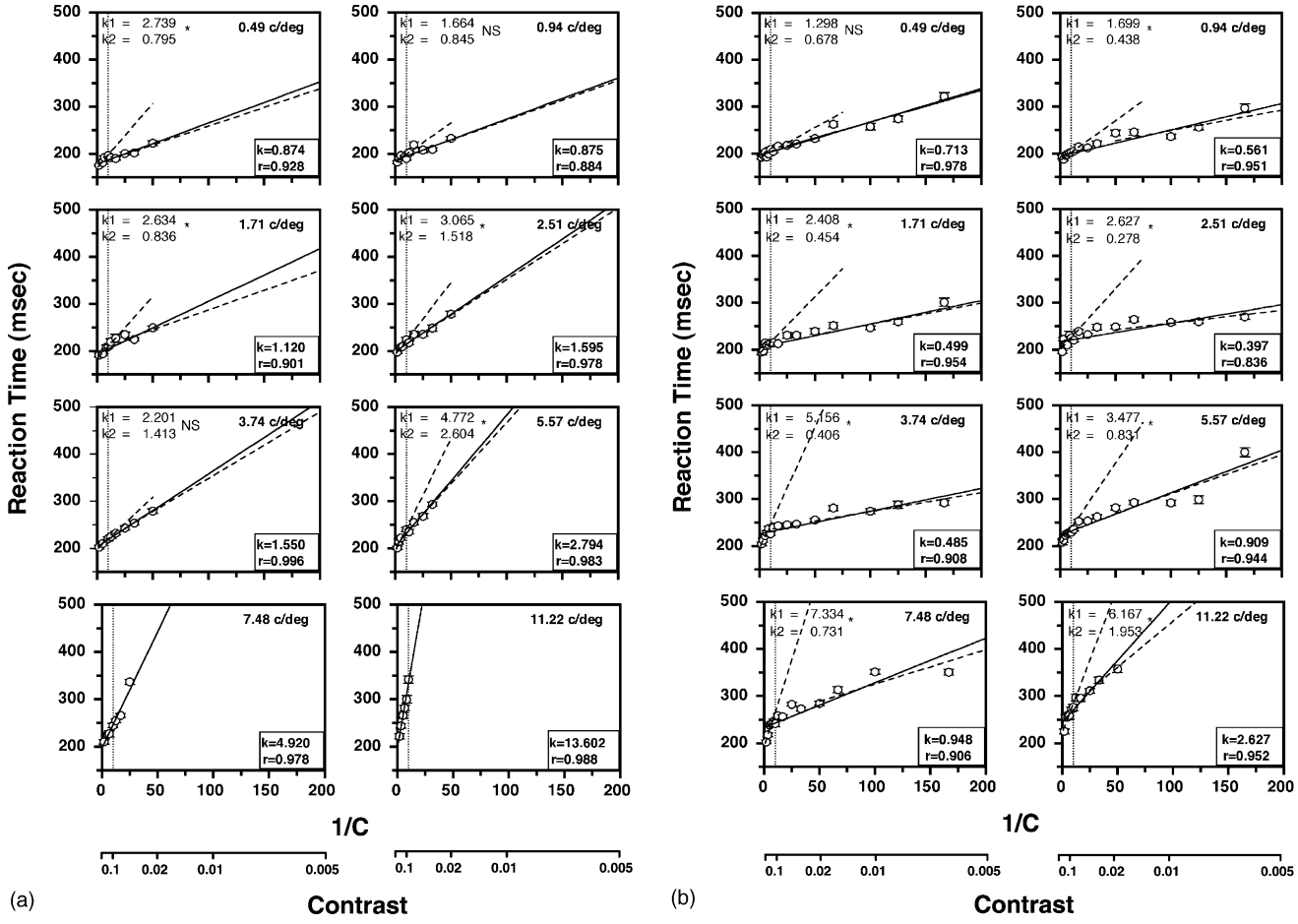

Fig. 3. (a) Plots of RT vs. the reciprocal of contrast ($1/C$) for a stimulus of 20 ms duration and for a range of spatial frequencies (subject SP). Mean screen luminance was 20 cd/m^2 and eccentricity 0 deg. Each data point represents the mean of 32 measurements and the error bars ±1 s.e. The solid lines represent the least squares regression fit for all the data points, whereas the dashed lines represent the least square regression fits for the two segments (i.e. high levels of contrast (0.5–0.1) and low levels of contrast (0.1 to threshold)). The legend indicates the spatial frequency of the grating used. Also, k is the slope for all the data points (solid line), r is the coefficient of determination and k_1 and k_2 are the slopes for high and low contrast levels (dashed lines), respectively. The asterisk indicates a statistical significance difference ($p < 0.05$) between k_1 and k_2; NS indicates no significant difference between the slopes. Only one slope is drawn when few data points ($\leqslant 6$) are plotted. (b) Plots of RT vs. the reciprocal of contrast ($1/C$) for a stimulus of 500 ms duration and for a range of spatial frequencies (subject SP). See (a) for detail.

function is bi-linear, the high contrast region of the curve always has a greater slope (i.e. low gain/sensitivity) than the low contrast region. In Fig. 3(a) (stimulus duration 20 ms) it is evident that the slope k_1 of the high contrast region does not change much with spatial frequency, but the slope k_2 of the low contrast region increases dramatically with spatial frequency. At the high spatial frequencies (7.48 and 11.22 c/deg) the RT vs. $1/C$ function is no longer bi-linear.

The longer duration data (Fig. 3(b)) are quite different. The high contrast slopes again do not change much with spatial frequency, but the break-point is evident even at the highest spatial frequencies, whereas it is absent for these frequencies for the shorter duration (Fig. 3(a)). It is clear that the slope of the low contrast region is particularly affected by the change in stimulus duration, as if it represents the activity of a mechanism whose sensitivity is influenced by changes in the temporal frequency content of the stimulus. This observation and its explanation are considered in Section 4.

The statistical significance of the change in slope between k_1 and k_2 was obtained as follows. The null hypothesis that the regression co-efficients k_1 and k_2 are equal ($k_1 - k_2 = 0$) was tested using the students t distribution, where $t = (k_1 - k_2)/S_{\text{res}}$ for $(n_1 + n_2) - 4$ degrees of freedom, n_1 and n_2 are the numbers of data points in the lower and upper segments of the line and S_{res} is the common residual variance for the two segments. Slopes were considered significantly different when $P < 0.05$. These cases are indicated by an asterisk in the figures. In many cases the break point between the two putative segments occurred at $C = 0.1$ and was obvious from visual inspection. When the selection of the break point was ambiguous, common residual variances were calculated for a sequence of points either side of $C = 0.1$. The break point giving the lowest

common residual variance for the two groups of data points was adopted as the break point. In all cases, this corresponded either to $C = 0.1$ or the data point immediately above or below this.

We now consider the effect of stimulus eccentricity. Fig. 4 illustrates how RT varies with horizontal eccentricity for two subjects, SP (Fig. 4(a)) and NH (Fig. 4(b)) for a spatial frequency of 5.57 c/deg. The uppermost panel in Fig. 4(a) and (b) shows the data for central fixation. There is an obvious break-point at around $C = 0.1$ and the low contrast region has a much shallower slope (0.593 for SP, 0.972 for NH) than the high contrast region (6.851 for SP, 3.903 for NH), again revealing the presence of two mechanisms. The panels below are displayed in pairs showing data for 5, 10 and 15 deg eccentricity with the left-hand panel showing the data presented to the left hemifield and the right-hand panel the data presented to the right hemifield. The data for both subjects show the same trend, with the slope of the low contrast region increasing at 5 deg until it coincides with the high contrast slope at 10 deg, when the break disappears. This probably indicates that only a single mechanism operates at higher eccentricities.

In Fig. 5, RTs vs. $1/C$ plots are drawn for low luminance (0.02 cd/m^2) for a range of spatial frequencies and for two subjects (SP and LG). Again, it is clear that the slope, k, becomes steeper (sensitivity decreases) as spatial frequency increases. Note, that the slopes are much steeper compared with those at 20 cd/m^2 (see Figs. 3 and 4), presumably because at low luminance levels sensitivity is low and small changes in contrast produce stronger effects on RT. Furthermore, there is no evi-

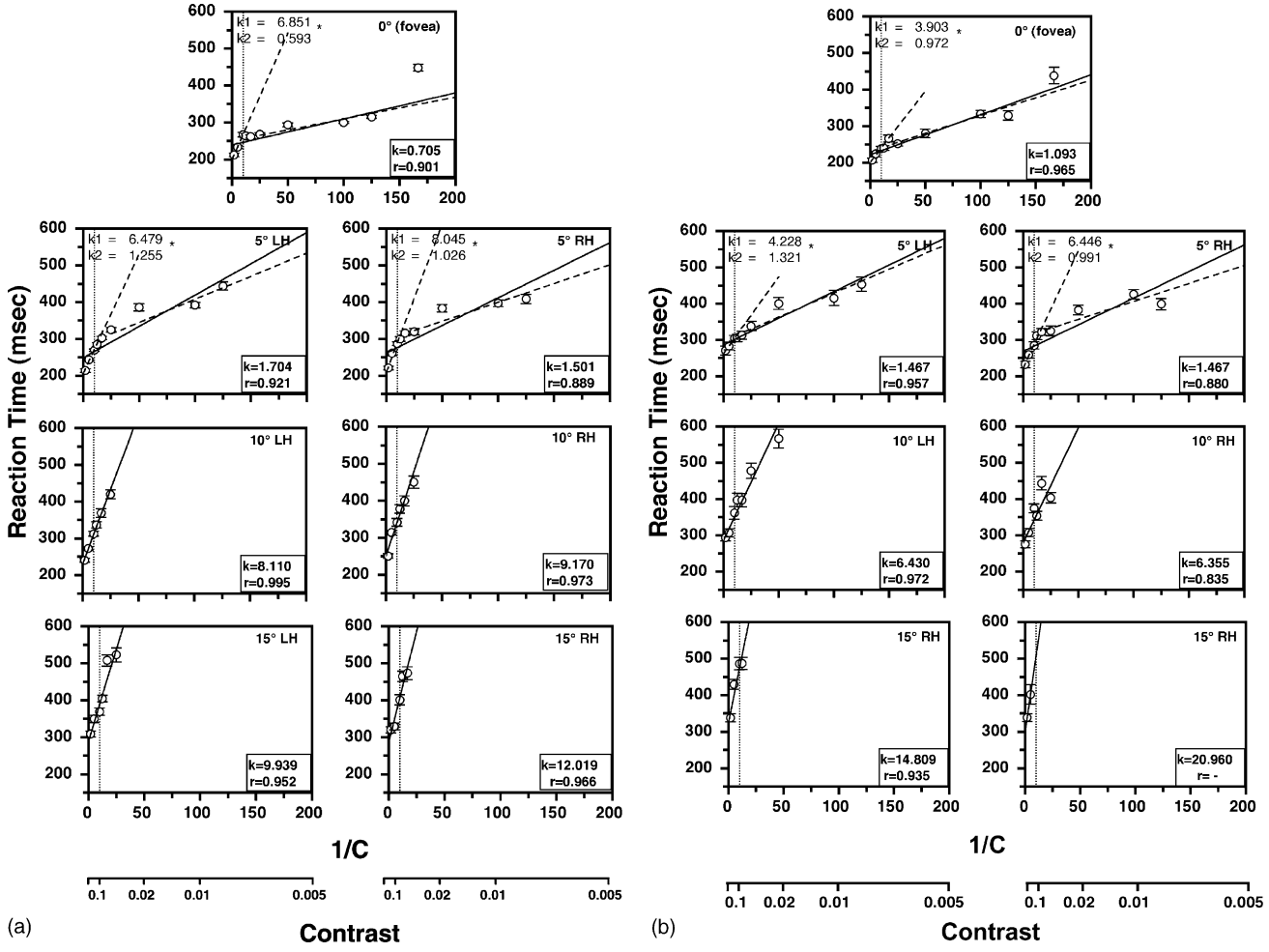

Fig. 4. (a) Plots of RT vs. the reciprocal of contrast ($1/C$) for a range of stimulus eccentricities (subject SP). The spatial frequency of the grating was 5.57 c/deg, the stimulus duration 340 ms and the mean screen luminance 20 cd/m^2. Each data point represents the mean of 32 measurements and the error bars ±1 s.e. The solid lines represent the least squares regression fit for all the data points, whereas the dashed lines represent the least square regression fits for the two segments (i.e. high levels of contrast (0.5–0.1) and low levels of contrast (0.1 to threshold)). The legend indicates the eccentricity used (LH: Left Hemifield, RH: Right Hemifield). Also, k is the slope for all the data points (solid line), r is the coefficient of determination and k_1 and k_2 are the slopes for high and low contrast levels (dashed lines), respectively. The asterisk indicates a statistical significance difference ($p < 0.05$) between k_1 and k_2; NS indicates no significant difference between the slopes. Only one slope is drawn when few data points ($\leqslant 6$) are plotted. (b) Plots of RT vs. the reciprocal of contrast ($1/C$) for a range of stimulus eccentricities (subject NH). See (a) for detail.

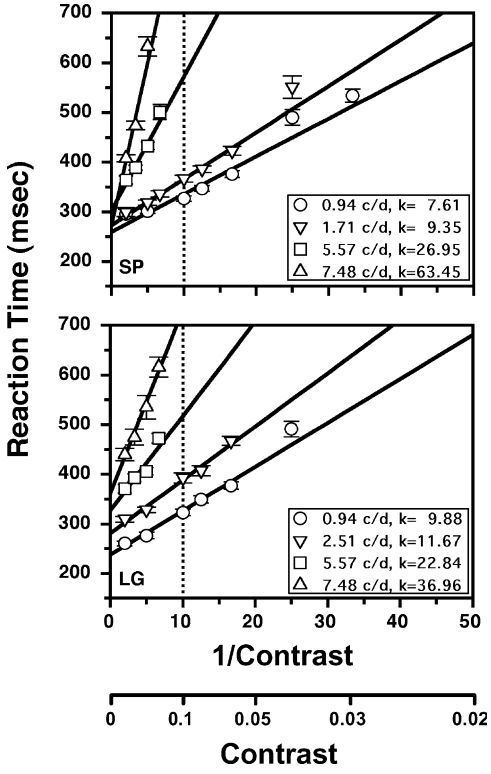

Fig. 5. Plots of RT vs. the reciprocal of contrast ($1/C$) for a range of spatial frequencies at a luminance of 0.02 cd/m^2 and for two subjects (SP: upper graph, LG: lower graph). Stimulus duration was 340 ms. Each data point represents the mean of 32 measurements and the error bars ±1 s.e. The solid lines represent the least squares regression fits. The dotted line indicates $C = 0.1$.

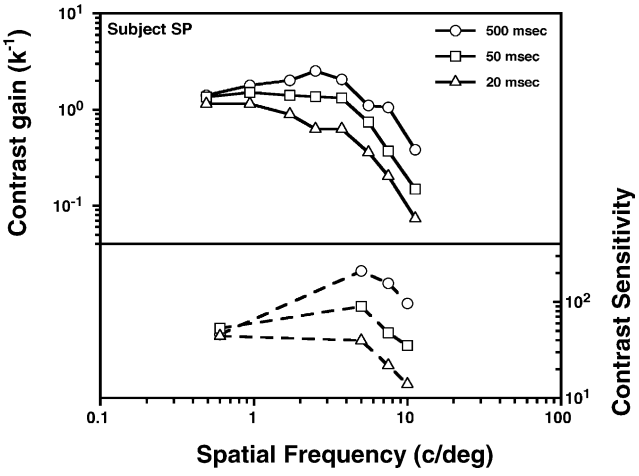

Fig. 6. Plots of the RT-based contrast gain (k^{-1}) (left axis) as a function of spatial frequency for a range of stimulus durations (500 ms—circles, 50 ms—squares, 20 ms—triangles) for one subject compared to contrast sensitivity data (right axis) from Kulikowski's (1971) study.

dence of a break above and below $C = 0.1$, suggesting that the same mechanism operates over the entire contrast range at this luminance level.

The figures so far described show that the slope, k, varies systematically with stimulus duration, eccentricity, luminance and spatial frequency. In the following figures, the RT-based contrast sensitivity (k^{-1}) is compared with conventional threshold-based contrast sensitivities.

The upper panel of Fig. 6 is a summary of the RT data plotted in terms of sensitivity (k^{-1}) and stimulus onset duration for a range of spatial frequencies (k is the *overall* slope of the RT function illustrated in Fig. 3(a) and (b)). Three durations, 20, 50 and 500 ms were tested. It is clear that for the long duration (500 ms) the spatial tuning of k^{-1}, is band-pass; it is reduced at the lower spatial frequencies, reaches a maximum at 2.51 c/deg and then decreases rapidly. The 50 ms duration data do not show such low frequency attenuation in $1/k$ and the 20 ms duration data show no band-pass characteristics at all, only a steady increase in $1/k$ as spatial frequency is decreased. In the lower panel the effects of stimulus duration on contrast sensitivity (redrawn from Kulikowski, 1971) are illustrated. These data exhibit the same pattern as the RT data. The shorter duration (20 ms) sensitivity function is low pass, whereas the longer duration (500 ms) function is band-pass.

In Fig. 7 the effect on RT of changing eccentricity is summarised. The upper panel depicts data from subject SP and the lower from subject NH. In Fig. 4 only one luminance was displayed whereas here we present data for three luminances, 20 cd/m^2 (solid lines), 0.2 cd/m^2 (dotted lines) and 0.02 cd/m^2 (dashed lines) and three spatial frequencies (0.49, 1.71 and 5.57 c/deg). Note that 0.2 cd/m^2 data are shown for SP only. Data from the left and right hemifields are shown either side of zero eccentricity. It is evident that, as in Fig. 6, k^{-1} adopts the shape of the contrast sensitivity function (CSF) as it varies with eccentricity (Johnson, Keltner, & Balestrery, 1978; Pointer & Hess, 1989; Robson & Graham, 1981). At 20 cd/m^2 (solid lines) it is maximal at the fovea and decreases approximately linearly with eccentricity. Under mesopic conditions (0.2 cd/m^2), k^{-1} remains largely independent of eccentricity, when low spatial frequencies (0.49 and 1.71 c/deg) are used. Note that the functions are symmetrical for the two hemifields (see also Holmes, Plainis, & Murray, 2000).

Finally, in Fig. 8 the spatial tuning of k^{-1} for a wide range of luminances is shown (subjects SP and LG). For both subjects the high luminance (20 cd/m^2) data exhibit band-pass characteristics. As luminance is reduced the function becomes low-pass and gain decreases. It is interesting to compare these data with the classical contrast sensitivity vs. luminance data of Van Nes and Bouman (1967) and Daitch and Green (1969). The overall effects of reducing luminance are qualitatively similar. The validity of this comparison is considered in Section 4.

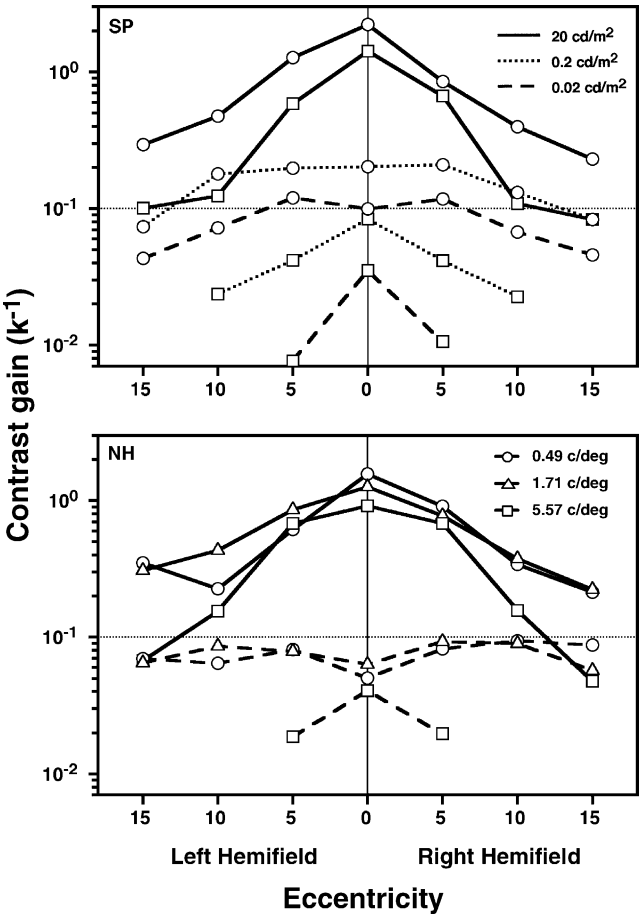

Fig. 7. Plots of the RT-based contrast gain (k^{-1}) as a function of eccentricity (both hemifields) for a range of spatial frequencies (0.49 c/deg—circles, 1.71 c/deg—triangles, 5.57 c/deg—squares) and luminances (20 cd/m^2—solid lines, 0.2 cd/m^2—dotted lines, 0.02 cd/m^2—dashed lines) and for two subjects (SP: upper panel, NH: lower panel).

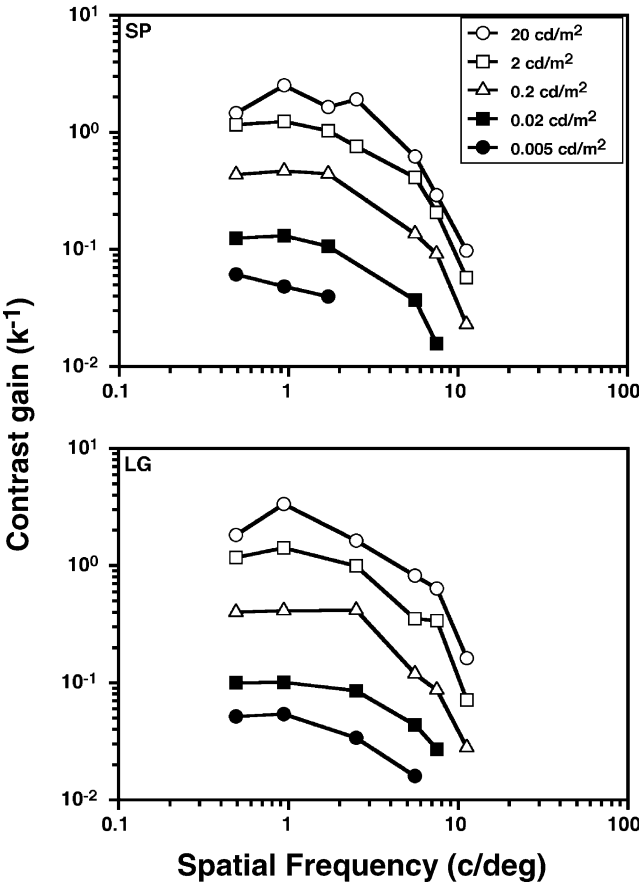

Fig. 8. Plots of the RT-based contrast gain (k^{-1}) as a function of spatial frequency for a range of luminances and for two subjects (SP: upper graph, LG: lower graph). The stimulus duration was 340 ms. Central fixation was used.

4. Discussion

In this paper we describe a series of experiments designed to characterise the processing of supra-threshold contrast using RTs. Recently, Plainis and Murray (2000) showed that for a wide range of stimulus conditions and all subjects tested, RTs can be plotted as a function of the reciprocal of contrast, to reveal a linear RT-contrast function. In the present study we extend these observations to a wider range of contrasts and demonstrate that, for conditions where sensitivity is high, a bi-linear RT-contrast function provides an improved fit to the data.

The transition point between the two slopes occurs at around $C = 0.1$. The segments above and below 0.1 are interpreted as revealing the activity of parvo and magno pathways, respectively. This suggests that RTs are regulated by the characteristics of neurons at the early stages of visual processing. In addition, it emerges that the bi-linear function may be present or absent, depending on sensitivity, for variations in eccentricity, luminance and duration of the grating stimulus. By taking the reciprocal of the slope of the RT vs. $1/C$ functions, k^{-1}, as a measure of sensitivity (gain), we show that close-to-threshold RTs reflect how contrast sensitivity varies with these parameters. This is consistent with the suggestion (Crook, Lange-Malecki, Lee, & Valberg, 1988; Kulikowski, 1989; Shapley & Hawken, 1999) that the M system forms the physiological substrate for most of the CSF, with the exception perhaps of the highest spatial frequencies.

4.1. RT-contrast functions reveal P and M processing

The bi-linear RT-contrast relationship (see Figs. 3 and 4), presented in this paper, offers new evidence regarding the physiological mechanisms underlying RTs and supra-threshold contrast coding. The discontinuity in the RT-contrast function between low and high contrast levels indicates a transition from M-dominated to P-dominated activity. At low contrasts, only a relatively small number of neurons, having high gain and fast responses (M cells) are activated. Increasing the contrast of the stimulus, recruits additional neurons (the

more numerous P cells) and thus reduces synaptic delay, probably via a probability summation mechanism. Moreover, M cells tend to saturate at high contrasts (Kaplan & Shapley, 1986). Therefore, it seems that the faster, high contrast branch of the bi-linear RT-contrast plot represents the contribution from a second population of neurons, the P cells.

There are three lines of evidence to support the above explanation. First, where there is a discontinuity, it falls close to contrast 0.1. It is well known that M cells are selectively activated at contrasts below 0.1. The evidence for this comes from many different types of experiments; Tootel, Hamilton, and Switkes (1988) showed that low contrast (<0.08) gratings produced de-oxyglucose staining only in the M projection to V1 macaque. Hicks et al. (1983) and many other authors (e.g. Derrington & Lennie, 1984; Kaplan & Shapley, 1986; Lee, Martin, & Valberg, 1989; Sclar et al., 1990) have used electrophysiological methods to show that P cells have much poorer sensitivity to luminance contrast than M cells for an extended range of spatial and temporal frequencies. It therefore seems unlikely that they subserve the low contrast RTs. Second, the RT-contrast functions show higher gain (shallow slopes in Fig. 3) at low contrasts and Kaplan and Shapley (1982) demonstrated that M cells have 10× higher gain than P cells. Third, the discontinuity is not present under all conditions; crucially, it is only obtained at low to moderate spatial frequencies and when sensitivity is high. When sensitivity is compromised (e.g. high spatial frequencies, low luminances, eccentric viewing) the gain of the underlying mechanism is low (steeper functions in Fig. 3), and the data can be fitted by a single function, which is likely to reflect the activity of a single mechanism or, as discussed below, the combined activity of P and M cells. This interpretation is also supported by the observation that, in the bi-linear RT-contrast plots, the slope of the low contrast branch becomes gradually steeper with increasing spatial frequency, until it coincides with that of the high contrast region.

It follows that under conditions where only a single mechanism is known to operate, a simple linear function should be obtained. This has been shown to be the case for RTs obtained from isoluminant chromatic stimuli which are processed exclusively by the P system (Burr & Corsale, 2001; Parry, 2001; Parry et al., 1988). Similarly, monophasic RT-contrast functions emerge when slow onset/offset stimuli are used (Parry, 2001), or when high spatial frequencies are tested (see Fig. 3(a) and (b); also Harwerth & Levi, 1978), where again detection is presumably mediated by a single mechanism, the P system, or perhaps combined activity of both systems (see below). On the other hand, low luminances (see Plainis & Murray, 2000) and parafoveal presentation (>5 deg) seems to favour a single system, presumably the M pathway (Thomas et al., 1999).

It is with the above argument in mind that we tested RTs at a series of different eccentricities and luminances. The dichotomy in the RT-contrast function is also present in the eccentricity data (at 5 deg; see Fig. 4), revealing again the presence of two mechanisms. The discontinuity disappears at greater eccentricities for 5.57 c/deg but remains at the lower spatial frequencies (0.49 and 1.71 c/deg) to 15 deg eccentricity (Holmes et al., 2000), because the sensitivity to low frequencies at these eccentricities is relatively high. When sensitivity decreases dramatically, as occurs for a 5.57 c/deg grating at 10–15 deg, a single RT-contrast function is obtained. This may reflect the activity of M-cells only. The important point is that sensitivity is reduced with eccentricity. This is due to pre-neural factors such as optics and the anatomical and directionall characteristics of the photoreceptors (Banks, Sekuler, & Anderson, 1991; Curcio, Sloan, Kalina, & Hendrickson, 1990; Lee, 1996; Malpeli, Lee, & Baker, 1996). Note that it has been claimed (Croner & Kaplan, 1995) that contrast gain of P cells increases in the periphery to counteract the blur introduced by optical aberrations.

We have shown in a previous paper (Plainis & Murray, 2000) that there is a gradual decrease in RT-based sensitivity with reducing luminance. A similar effect can be seen for all luminance levels as spatial frequency varies (see Figs. 3 and 6). Sensitivity gradually decreases with increasing spatial frequency, suggesting a slow transition between different underlying mechanisms. This transition may have its physiological basis in the overlap in M and P cells in the recipient layers (4c) of the striate cortex (V1). It has been known for some time that the segregation between M and P cells is incomplete (Kaplan & Shapley, 1982). More recently Lund et al. (1995) and Bauer et al. (1999) have shown that the terminal fields of both M and P thalamic axons exhibit substantial overlap within their respective α and β territories of layer 4C. In other words there is intrusion of P axon terminals in to 4Cα and of M axon terminals in to 4Cβ. This anatomical overlap is elegantly matched by functional overlap between the two systems. The receptive field size and contrast sensitivity of cells decrease gradually from the top to the bottom of 4C and it is tempting to speculate that this may be reflected in our RT data in the form of a gradually decreasing RT-based contrast gain with increasing spatial frequency. Functionally, the slow shift in emphasis from cells with parvo-like properties to cells with magno-like properties suggests that the P system exerts an increasing influence on contrast sensitivity as spatial frequency increases.

4.2. Bi-modality in VEP studies

The phenomenon of a bi-linear contrast function is not restricted to RT data. A dichotomy between two

systems has been reported in VEPs using rapidly flickering lights and gratings in humans (Baseler & Sutter, 1997; Hartwell & Cowan, 1993; Kubova, Kuba, Spekreijse, & Blakemore, 1995; Mihaylova et al., 1999; Murray & Kulikowski, 1983; Murray et al., 1987; Parry et al., 1988; Rudvin et al., 2000). The origin of these findings was firstly discussed in terms of psychophysical mechanisms (Mihaylova et al., 1999; Murray & Kulikowski, 1983; Regan, 1973), but in the light of the more recent understanding of early visual processing it seems likely that M and P pathways form the neural substrates of contrast dependency in the VEPs (Baseler & Sutter, 1997; Kubova et al., 1995; McKeefry, 2001; Murray & Parry, 1996; Rudvin et al., 2000). Like the contrast function of the M pathway, the low contrast region of the VEP vs. contrast function saturates at a relatively low contrast, of 0.1 (Baseler & Sutter, 1997; Hartwell & Cowan, 1993; Murray et al., 1987; Rudvin et al., 2000). The high contrast region exhibits a large dynamic range and saturates at a higher contrast. However, VEP-contrast functions are not as steep as RT-contrast functions (Hartwell & Cowan, 1993; Mihaylova et al., 1999; Vassilev, Mihaylova, & Bonnet, 2002), perhaps because they involve later stages of visual processing.

4.3. RTs and contrast sensitivity

There is little doubt that RTs are greatly influenced by the contrast sensitivity (gain) of the underlying detection mechanisms. It would be surprising if this were not the case, but precisely how RTs reflect the processing of supra-threshold contrast is less intuitively obvious. As indicated in Section 1, the RT paradigm is biased toward transient activity and the traditional methods for assessing supra-threshold perception, contrast matching and magnitude estimation (e.g. Blakemore, Muncey, & Ridley, 1973; Georgeson & Sullivan, 1975; Watanabe, Mori, Nagata, & Hiwatashi, 1968) probably reflect slow, sustained-type processes.

Figs. 3 and 4 illustrate that the overall slope, k, of the RT-contrast functions coincides with the slope, k_2, of the low contrast branch, which reflects M activity. If the RT-based contrast sensitivity data are qualitatively similar to conventional sensitivity measures, then this is further evidence that CSFs, at least for low and medium spatial frequencies are mediated by the M pathway.

4.3.1. Eccentricity

Fig. 7 shows that the high luminance (20 cd/m^2) RT-based sensitivity functions have a similar form to the corresponding CSFs (e.g. Pointer & Hess, 1989; Robson & Graham, 1981) there is a fall-off in sensitivity as eccentricity increases. Pointer and Hess (1989) found different gradients of sensitivity loss for gratings below and above 1 c/deg and our data agree with this in that the 5.57 c/deg RT data show a greater decline with eccentricity than the lower spatial frequencies. This may reflect a change in the ratio of P to M contribution with eccentricity, but can also be explained by the convergence of cone signals in the periphery (Curcio et al., 1990), which increases the diameter of the effective sampling unit. This and the reduction in retinal image quality reduce peripheral sensitivity to higher frequencies.

On the other hand, at intermediate (0.2 cd/m^2) and low (0.02 cd/m^2) luminances rod pathways dominate, resulting in long RTs and different eccentricity functions (see Fig. 7). At these luminance levels the RT-based contrast gain (for the 0.49 and 1.71 c/deg gratings) remains largely independent of eccentricity, suggesting that the same system mediates the response across the entire range. As expected, the poor spatial sampling by rods means that for 5.57 c/deg, RTs obtained for central fixation are shorter than those obtained with eccentric viewing.

The symmetry of these functions is particularly significant for the present report. We might expect that images processed relatively early in the visual pathway would be symmetrical. Identification (Kitterle, Christman, & Hellige, 1990) and discrimination (Niebauer & Christman, 1999; Proverbio, Zani, & Avella, 1997) tasks, or more complex images (Sergent, 1983), are known to have different RT functions when right and left hemispheres are compared. Hence, the symmetry of the hemifield data adds weight to the argument that the RTs obtained in our experiments are characteristic of information processing in the early stages of human vision.

4.3.2. Luminance

The raw data for RTs obtained under mesopic conditions show, as expected, only a low sensitivity monotonic function (Fig. 5). Here, though the detection of the stimulus is almost certainly due to the M pathway, the familiar poor temporal characteristics of low luminance vision, are reflected in dramatic increases in RTs as contrast is reduced. Again when these data are summarised and transformed in to sensitivity functions, there is a striking similarity with the classical change in shape of the CSFs from band pass to low pass as luminance is reduced as described by Van Nes and Bouman (1967). It is well known that the band-pass shape for achromatic contrast sensitivity occurs as a result of subtractive lateral inhibition (Donner & Hemila, 1996; Enroth-Cugell & Robson, 1966). At low luminances, the lateral inhibition is reduced and, for a given spatial frequency, grating contrast sensitivity increases in direct proportion to the square root of average luminance as described in the DeVries–Rose Law (DeVries, 1943; Rose, 1948). At higher luminances, Weber's law holds and contrast sensitivity is independent of luminance. As spatial frequency is increased, the transition luminance

between the two laws increases (Mustonen, Rovamo, & Nasanen, 1993).

In fact, though they are qualitatively similar, there are some differences between the RT-based sensitivity functions and the Van Nes and Bouman (1967) sensitivity data. In the RT-based data, the band pass shape is evident only at 20 cd/m^2 (c.500 td) for our subjects and when luminance is reduced to 2 cd/m^2 (approximately 60 td) the function becomes low pass. This is not the case for the Van Nes and Bouman threshold-based data. It has a band pass shape at quite low luminances (0.9 td) and becomes low pass only at 0.09 td. Hence RT-based sensitivity is excessively reduced with luminance at the lowest spatial frequency and for quite moderate luminances. In other words, it is more susceptible to reductions in luminance than the threshold function. The change from band-pass to low-pass shape represents the transition from Weber's law to the DeVries–Rose Law. This effect, of RTs being disproportionately affected by luminance compared with the equivalent sensitivity data, forms part of a separate study.

4.3.3. Presentation time

As shown by Kulikowski (1971) and Harris and Georgeson (1986), reducing the presentation time of gratings results in a low pass rather than the more familiar band-pass shape. We show in Fig. 6 that this fundamental change in shape of the CSF between long (500 ms) and short (20 ms) duration stimuli is mirrored in RT data. The similarities with the threshold-based data, re-plotted from Kulikowski (1971) are striking. It would appear that RT-based gain derived at relatively low spatial frequencies, such as 0.6 and 1 c/deg, is independent of stimulus duration. As spatial frequency increases, the duration effects become stronger, and shorter durations give rise to reduced sensitivity, both in terms of contrast sensitivity and RTs. Note that each data point in the upper panel of Fig. 6 is based on a range of contrasts from threshold to maximum contrast, thus the data imply that, for RTs, the processing of supra-threshold contrast follows closely the CSF.

As a general point it should be emphasised that the stimuli used in these experiments are vertical sinusoidal gratings and the task is a simple RT measure. The extent to which the neurophysiological characteristics of the visual pathway affect RTs is strongly dependent on the type of stimulus used and the complexity of the task. In some cases, for example choice RTs, cognition and higher levels of visual processing influence the data, whereas in the experiments presented in this paper, the response is closely linked to detection. It seems likely that when complex images are used, or when uncertainty effects such as close-to-threshold stimuli are introduced, RTs will have a sensory and a cognitive component. In these cases, contrast, duration and eccentricity may be confounding variables and should therefore be carefully controlled.

5. Concluding comments

The bi-linear RT-contrast function is central to this paper. Showing when it occurs and when it does not, reveals the activity of underlying mechanisms having different contrast gain. Comparisons between human and neurophysiological data must be made with caution, but there can be little doubt that the bi-linear function represents the activity of separate mechanisms. Hence the results reinforce current neurophysiology; when there are two functions, the M system dominates close-to-threshold RTs, whereas the P system takes over at higher contrasts, mainly because of the saturation of the M system.

The simple linear relationship indicates that either a single mechanism, P or M depending on stimulus conditions, operates over the whole contrast range. As speculated above, there may be conditions where detection is mediated by cells, located in the overlap region of layer 4C in V1, having both P-like and M-like properties. This would explain the systematic sensitivity (gain) change with spatial frequency in Figs. 3 and 5.

Finally, when RT data are transformed in to spatial sensitivity functions of presentation time, luminance or eccentricity, they are qualitatively similar to the corresponding threshold-based sensitivity measures. This supports the notion that the M system is primarily responsible for close-to-threshold detection and probably forms the basis of the CSF.

Acknowledgements

Sotiris Plainis was funded by the EPSRC under the LINK IST scheme. The industrial partners were WRTL Exterior Lighting Ltd. and Dolland and Aitchison Ltd. We gratefully acknowledge Janus Kulikowski for many useful remarks on an early version of the paper. We thank one referee unreservedly for clarifying a critical point.

References

Banks, M. S., Sekuler, A. B., & Anderson, S. J. (1991). Peripheral spatial vision: limits imposed by optics, photoreceptors, and receptor pooling. *Journal of Optical Society of America A, 8*, 1775–1787.

Baseler, H. A., & Sutter, E. E. (1997). M and P components of the VEP and their visual field distribution. *Vision Research, 37*, 675–690.

Bauer, U., Scholz, M., Levitt, J. B., Obermayer, K., & Lund, J. S. (1999). A model for the depth-dependence of receptive field size and contrast sensitivity of cells in layer 4C of macaque striate cortex. *Vision Research, 39*, 613–629.

Blakemore, C., Muncey, J. P. J., & Ridley, R. M. (1973). Stimulus specificity in the human visual system. *Vision Research, 13*, 1915–1931.

Breitmeyer, B. G. (1975). Simple reaction time as measure of the temporal response properties of transient and sustained channels. *Vision Research, 15*, 1141–1142.

Burbeck, C. A., & Kelly, D. H. (1981). Contrast gain measurements and the transient/sustained dichotomy. *Journal of the Optical Society of America A, 71*, 1335–1342.

Burkhardt, D. A., Gottesman, J., & Keeman, R. M. (1987). Sensory latency and reaction time: dependence on contrast polarity and early linearity in human vision. *Journal of the Optical Society of America A, 4*, 530–539.

Burr, D. C., & Corsale, B. (2001). Dependency of reaction times to motion onset on luminance chromatic contrast. *Vision Research, 41*, 1039–1048.

Croner, L. J., & Kaplan, E. (1995). Receptive fields of P and M ganglion cells across the primate retina. *Vision Research, 35*, 7–24.

Crook, J. M., Lange-Malecki, B., Lee, B. B., & Valberg, A. (1988). Visual resolution of macaque retinal ganglion cells. *Journal of Physiology, 396*, 205–224.

Curcio, C. C., Sloan, K. R., Kalina, R. E., & Hendrickson, A. E. (1990). Human photoreceptor topography. *The Journal of Comparative Neurology, 292*, 497–523.

Daitch, J. M., & Green, D. G. (1969). Contrast sensitivity of the human peripheral retina. *Vision Research, 9*, 947–952.

Derrington, M., & Lennie, P. (1984). Spatial and temporal contrast sensitivity of neurones in lateral geniculate nucleous of macaque. *Journal of Physiology, 357*, 219–240.

DeVries, H. L. (1943). The quantum character of light and its bearing upon threshold of vision, the differential sensitivity and visual acuity of the eye. *Physica, 10*, 553–564.

Donner, K., & Hemila, S. (1996). Modelling the spatio-temporal modulation response of ganglion cells with difference-of-Gaussians receptive fields: Relation to photorecpetor response kinetics. *Visual Neuroscience, 13*, 173–186.

Enroth-Cugell, C., & Robson, J. C. (1966). The contrast sensitivity of retinal ganglion cells of the cat. *Journal of Physiology, 187*, 517–552.

Felipe, A., Buades, M. J., & Artigas, J. M. (1993). Influence of the contrast sensitivity function on reaction time. *Vision Research, 33*, 2461–2466.

Gegenfurtner, K. R., & Hawken, M. J. (1996). Interaction of motion and color in the visual pathways. *Trends in Neurosciences, 19*, 394–401.

Georgeson, M. A., & Sullivan, G. D. (1975). Contrast constancy: deblurring in human vision by spatial frequency channels. *Journal of Physiology, 252*, 627–656.

Harris, M. G., & Georgeson, M. A. (1986). Sustained and transient temporal integration functions depend on spatial frequency, not grating area. *Vision Research, 26*, 1779–1782.

Hartwell, R. C., & Cowan, J. D. (1993). Evoked potentials and simple motor reaction times to localised visual patterns. *Vision Research, 33*, 1325–1337.

Harwerth, R. S., Boltz, R. L., & Smith III, E. L. (1980). Psychophysical evidence for sustained and transient channels in the monkey visual system. *Vision Research, 20*, 15–22.

Harwerth, R. S., & Levi, D. M. (1978). Reaction time as a measure of suprathreshold grating detection. *Vision Research, 18*, 1579–1586.

Hicks, T. P., Lee, B. B., & Vidyasagar, T. R. (1983). The responses of cells in macaque lateral geniculate nucleous to sinusoidal gratings. *Journal of Physiology, 337*, 183–200.

Holmes, N. P., Plainis, S., & Murray, I. J. (2000). Reaction Times as a behavioural measure of contrast gain; comparison of low and high luminance levels and different eccentricities. *Perception, 29*(Suppl.), 78.

Johnson, C. A., Keltner, J. L., & Balestrery, F. (1978). Effects of target size and eccentricity on visual detection and resolution. *Vision Research, 18*, 1217–1222.

Kaplan, E., Lee, B. B., & Shapley, R. M. (1990). New views of primate retinal function. In N. Osborne, & G. Chader (Eds.), *Progress of retinal research* (pp. 273–336). Oxford: Pergamon Press.

Kaplan, E., & Shapley, R. M. (1982). X and Y cells in the lateral geniculate nucleous of macaque retina. *Journal of Physiology, 330*, 125–143.

Kaplan, E., & Shapley, R. M. (1986). The primate retina contains two types of ganglion cells, with high and low contrast sensitivity. *Proceedings of National Academy of Science USA, 83*, 2755–2757.

Kitterle, F. L., Christman, S., & Hellige, J. B. (1990). Hemispheric differences are found in the identification, but not detection, of low versus high spatial frequencies. *Perception and Psychophysics, 48*, 297–306.

Kubova, Z., Kuba, M., Spekreijse, H., & Blakemore, C. (1995). Contrast dependence of motion-onset and pattern-reversal evoked potentials. *Vision Research, 35*, 197–205.

Kulikowski, J. J. (1971). Some stimulus parameters affecting spatial and temporal resolution of human vision. *Vision Research, 11*, 83–93.

Kulikowski, J. J. (1989). The role of P and M systems: (c) psychophysical aspects. In J. J. Kulikowski, C. M. Dickinson, & I. J. Murray (Eds.), *Seeing contour and colour* (pp. 232–237). Oxford: Pergamon Press.

Lee, B. B. (1996). Receptive field structure in the primate retina. *Vision Research, 36*, 631–644.

Lee, B. B., Martin, P. R., & Valberg, A. (1989). Sensitivity of macaque retinal ganglion cells to chromatic and luminance flicker. *Journal of Physiology, 424*, 223–243.

Lee, B. B., Pokorny, J., Smith, V. C., Martin, P. R., & Valberg, A. (1990). Luminance chromatic modulation sensitivity of macaque ganglion cells and human observers. *Journal of the Optical Society of America A, 7*, 2223–2237.

Legge, G. (1978). Sustained and transient mechanisms in human vision: temporal and spatial properties. *Vision Research, 18*, 69–81.

Lund, J. S., Wu, Q., Hadingham, P. T., & Levitt, J. B. (1995). Cells and circuits contributing to functional properties in area V1 of macaque monkey cerebral cortex: Bases for neuroanatomically realistic models. *Journal of Anatomy, 187*, 563–581.

Lupp, U., Hauske, G., & Wolf, W. (1976). Perceptual latencies to sinusoidal gratings. *Vision Research, 16*, 969–972.

Malpeli, J. G., Lee, D., & Baker, F. H. (1996). Laminar and retinotopic organization of the macaque lateral geniculate nucleus: magnocellular and parvocellular magnification functions. *The Journal of Comparative Neurology, 375*, 363–377.

Mansfield, R. J. W. (1973). Latency functions in human vision. *Vision Research, 13*, 2219–2234.

McKeefry, D. J. (2001). Visual evoked potentials elicited by chromatic motion onset. *Vision Research, 41*, 2005–2025.

Menees, S. M. (1998). The effect of spatial frequency adaptation on the latency of spatial contrast detection. *Vision Research, 38*, 3933–3942.

Mihaylova, M., Stomonyakov, V., & Vassilev, A. (1999). Peripheral and central delay in processinf high spatial frequencies: reaction time and VEP latency studies. *Vision Research, 39*, 699–705.

Murray, I. J., & Kulikowski, J. J. (1983). VEPs and Contrast. *Vision Research, 23*, 1741–1743.

Murray, I. J., & Parry, N. R. A. (1996). Generating VEPs specific to Parvo and Magno pathways in humans. In C. M. Dickinson, I. J. Murray, & D. Carden (Eds.), *John Dalton's colour vision legacy* (pp. 471–477). Taylor and Francis.

Murray, I. J., & Parry, N. R. A. (1998). Assymetry of on and off reponses in transient pattern detection. *Investigative Ophthalmology and Vision Science, 39*(Suppl.), S410.

Murray, I. J., Parry, N. R. A., Varden, D., & Kulikowski, J. J. (1987). Human visual evoked potentials to chromatic and achromatic gratings. *Clinical Vision Sciences, 1*, 231–244.

Murray, I. J., & Plainis, S. (2000). A general equation for reaction times to contrast, spatial frequency and luminance. *Investigative Ophthalmology and Visual Science, 41*(4), S802.

Musselwhite, M. J., & Jeffreys, D. A. (1985). The influence of spatial frequency on the reaction times and evoked potentials recorded to grating pattern stimuli. *Vision Research, 25*, 1545–1555.

Mustonen, J., Rovamo, J., & Nasanen, R. (1993). The effect of grating area and spatial frequency on contrast sensitivity as a function of light level. *Vision Research, 33*, 2065–2072.

Niebauer, C. L., & Christman, S. D. (1999). Visual differences in spatial frequency discrimination. *Brain and Cognition, 41*, 381–389.

Parker, D. M. (1980). Simple reaction times to the onset, offset, and contrast reversal of sinusoidal grating stimuli. *Perception and Psychophysics, 28*, 365–368.

Parry, N. R. A. (2001). Contrast dependency of reaction times to chromatic gratings. *Color Research and Application, 26*, S161–164.

Parry, N. R. A., Kulikowski, J. J., Murray, I. J., Kranda, K., & Ott, H. (1988). Visual evoked potentials and reaction times to chromatic and achromatic stimulation: Psychopharmacological applications. In I. Hindmarch, B. Aufdembrinke, & H. Ott (Eds.), *Psychopharmacology and reaction times* (pp. 155–176). Chichester: Wiley.

Perry, V. H., Oehler, R., & Cowey, A. (1984). Retinal ganglion cells that project to the dorsal lateral geniculate nucleous in the macaque monkey. *Neuroscience, 12*, 1110–1123.

Piéron, H. (1952). *The sensations*. London: Frederick Muller Ltd.

Pins, D., & Bonet, C. (2000). The Piéron function in the threshold region. *Perception and Psychophysics, 62*, 127–136.

Plainis, S., & Murray, I. J. (2000). Neurophysiological interpretation of human visual reaction times: effect of contrast, spatial frequency and luminance. *Neuropsychologia, 38*, 1555–1564.

Pointer, J. S., & Hess, R. F. (1989). The contrast sensitivity gradient across the human visual field: with emphasis on the low spatial frequency range. *Vision Research, 29*, 1133–1151.

Pokorny, J., & Smith, V. C. (1997). Psychophysical signatures associated with magnocellular and parvocellular pathway contrast gain. *Journal of the Optical Society of America A, 14*, 2477–2486.

Proverbio, A. M., Zani, A., & Avella, C. (1997). Hemispheric asymmetries for spatial frequency discrimination in a selective attention task. *Brain and Cognition, 34*, 311–320.

Purpura, K., Kaplan, E., & Shapley, R. M. (1988). Background light and the contrast gain of primate P and M retinal ganglion cells. *Proceedings of National Academy of Science USA, 85*, 4534–4537.

Purpura, K., Tranchina, D., Kaplan, E., & Shapley, R. M. (1990). Light adaptation in the primate retina: Analysis of changes in gain and dynamics of monkey retinal ganglion cells. *Visual Neuroscience, 4*, 75–93.

Regan, D. (1973). An evoked potential correlate of colour: evoked potential findings and single-cell speculation. *Vision Research, 13*, 1933–1941.

Robson, J. G., & Graham, N. (1981). Probability summation and regional variation in contrast sensitivity across the visual field. *Vision Research, 21*, 409–418.

Rodieck, R. W., Binmoeller, K. F., & Dineen, J. (1985). Parasol and midget ganglion cells of the human retina. *Journal of Comparative Neurology, 233*, 115–132.

Rose, A. (1948). The sensitivity performance of the human eye on an absolute scale. *Journal of the Optical Society of America, 38*, 196–208.

Rudd, M. E. (1988). Quantal fluctuation limitations on reaction time to sinusoidal gratings. *Vision Research, 28*, 179–186.

Rudvin, I., Valberg, A., & Kilavik, B. E. (2000). Visual evoked potentials and magnocellular and parvocellular segregation. *Visual Neuroscience, 17*, 579–590.

Schwartz, S. H. (1992). Reaction time distributions and their relationship to the transient/sustained nature of the neural discharge. *Vision Research, 32*, 2087–2092.

Sclar, G., Maunsell, J. H. R., & Lennie, P. (1990). Coding of image contrast in central visual pathways of the macaque monkey. *Vision Research, 30*, 1–100.

Sergent, J. (1983). Role of the input in visual hemispheric asymmetries. *Psychological Bulletin, 93*, 481–512.

Shapley, R. M., & Hawken, M. J. (1999). Parallel retino-cortical channels and luminance. In K. R. Gegenfurtner, & L. T. Sharpe (Eds.), *Color Vision: from pigments to perception* (pp. 221–234). Cambridge: Cambridge University Press.

Thomas, J. P., Fagerholm, P., & Bonnet, C. (1999). One spatial filter limits speed of detecting low and middle spatial frequencies. *Vision Research, 39*, 1683–1693.

Tolhurst, D. J. (1975). Reaction times in the detection of gratings by human observers: a probalistic mechanism. *Vision Research, 15*, 1143–1149.

Tootel, R. B. H., Hamilton, S. L., & Switkes, E. (1988). Functional anatomy of macaque striate cortex. IV Contrast and magno-parvo streams. *Journal of Neuroscience, 8*, 1594–1609.

Totev, C., & Mitov, D. (2000). Temporal integration and reaction time to grating-onset detection. *Perception, 29*(Suppl.), 61.

Van Nes, F. L., & Bouman, M. A. (1967). Spatial modulation transfer in the human eye. *Journal of Optical Society of America, 57*, 401–406.

Vassilev, A., Mihaylova, M., & Bonnet, C. (2002). On the delay in processing high spatial frequency visual information: reaction time and VEP study of the effect of local intensity of stimulation. *Vision Research, 42*, 851–864.

Vassilev, A., & Mitov, D. (1976). Perception and spatial frequency. *Vision Research, 16*, 89–92.

Watanabe, A., Mori, T., Nagata, S., & Hiwatashi, K. (1968). Spatial sine-wave responses of the human visual system. *Vision Research, 8*, 1245–1263.

Wiesel, T. N., & Hubel, D. H. (1966). Spatial and chromatic interactions in the lateral geniculate body of the rhesus monkey. *Journal of Neurophysiology, 29*, 1115–1156.

Yeh, T., Lee, B. B., & Kremers, J. (1995). Temporal response of ganglion cells of the macaque retina to cone-specific modulation. *Journal of the Optical Society of America A, 12*, 456–464.